# A ZigBee-based wireless system for monitoring vital signs in hyperbaric chambers: Technical report

Cristian Carmona MSc [1], Bartomeu Alorda PhD [1], Luis Gracia PhD [2], Carlos Perez-Vidal PhD [3], Antonio Salinas MSc [3]

[1] Illes Balears University, Ctra, Valldemossa km 7.5 Ed. Mateu Orfila, 07122 Palma, SPAIN
[2] Instituto IDF, Universitat Politecnica de Valencia, 46022 Valencia, SPAIN
[3] Miguel Hernández University 03202 Elche, SPAIN

CORRESPONDING AUTHOR: Luis Gracia Ph.D. – *luigraca@isa.upv.es*

## ABSTRACT

This paper presents the replacement of a traditional wired communication link of the hyperbaric chambers with a wireless ZigBee-based system. This move allows a reduction in the costs of seals capable of withstanding the internal pressures and gives rise to a more versatile system. The new system is able to capture and process individual vital signs like the electrocardiography signal, and other analog sources, sending the data to an external computer and allowing analysis, representation and sharing with medical staff. This system solves such problems as the attenuation of the signal produced by the metal walls of the hyperbaric chamber and has a coverage area large enough to manage up to six patients with an effective data rate conversion of 2kHz. Furthermore, a battery-based and multiparameter platform is designed for multipatient hyperbaric chambers.

## 1. INTRODUCTION

The practice of hyperbaric medicine consists of using oxygen at a higher level than atmospheric pressure in order to increase the level of the oxygen in blood and thereby dissolve nitrogen bubbles [1]. Traditionally this technique has been used to treat diving disorders, decompression sickness and gas embolism. For this purpose, hyperbaric chambers (HC) – sealed vessels with a forced supply of air to increase the pressure inside – are used.

Hyperbaric oxygen ($HBO_2$) is used in a number of therapies such as treating carbon monoxide poisoning [2], air/gas embolism [3], delayed radiation injury [4] and enhancement of healing in selected problem wounds. In this sense, the numbers of patients receiving $HBO_2$ therapy are increasing. Because of this growth, new systems are required to improve the security, the efficiency and the costs of medical instrumentation. This paper proposes the installation of a wireless system inside the HC. Its purpose: to improve HC versatility and user mobility inside the chamber by reducing the number of cables from the inside to the outside.

The solution proposed by Lin, et al. [5] uses peer-to-peer communication architecture. This type of approach lacks traffic network monitoring and management capabilities and, hence is not suitable when the number of emitters and receivers increase. The number of patients impacts directly on the interference level and the signal quality, reducing the radio link capacity. The solution proposed by Hu, et al. [6] uses a Bluetooth-based platform to wirelessly transmit vital signs remotely. This approach considers a network architecture with a short-range radio transceiver, which is not suitable for HC environments since communications capability outside the vessel is limited. A commercial device based on Bluetooth technology has been evaluated in this paper to estimate the coverage area. In particular, the Shimmer Wireless Electrocardiogram (ECG) Sensor [7] was tested in a hyperbaric environment, but signal coverage was extremely reduced and the receiver had to be affixed to one of the HC windows in order to properly detect the signals.

Originally, Bluetooth-based solutions [8, 9] have been

KEYWORDS: computer-related health issues; medical information systems; low-power design

| wireless solution | coverage | transmission rate | patient number impact | battery power |
|---|---|---|---|---|
| IEEE802.15.4 [10] | 2 | 2 | 4 | 4 |
| Bluetooth [6, 7] | 1 | 1 | 3 | 4 |
| WiFi [8, 9] | 4 | 4 | 1 | 1 |
| ZigBee (proposed) | 3 | 3 | 2 | 4 |

**TABLE 1.** Comparison of wireless solutions for HC (scores 4 and 1 are for best and worst solution, respectively).

used for long-term monitoring for personal in-home health care, using a high-rate communications platform like IEEE802.1.15 or 3G/GSM to transmit information to the receiver. Although these approaches offer good transmission quality, transmitters with high power consumption require higher battery demands or continuous-power supply plugs not available within the HC. The system proposed by Chung, et al. [10] is the IEEE802.15.4-based communication platform working on self-designed hardware. However, the configuration of the sensors does not suit the typical requirements for HC applications, as discussed below.

First, an elevated number of patients will need monitoring, so the number of wireless nodes will be large if each person has one radio emitter for each sensor (a concentrator system and one radio emitter per person would be more efficient). Next, it is expected that communications will have high interference levels between nodes since the metal composition of HC walls acts like a signal repeater, increasing radio frequency noise. Finally, the hyperbaric atmosphere and high-pressure conditions are not considered in the enclosure design of that particular solution.

From the analysis of previous solutions and taking into account the low coverage area obtained with the commercial platforms based on Bluetooth protocol, a self-solution, as described in this paper, has been developed to solve the particular problem of the Perpetuo Socorro Hospital, located in Alicante, Spain.

This paper proposes a low-power battery-based solution using the ZigBee network [11] to transmit several health parameters – including the ECG signal – which is captured using a three-point differential measurement.

**FIGURE 1.** Hyperbaric chamber used in the work described in this paper: inside view (top); external view with detail of windows.

This battery-based solution helps to adapt the devices to multiple uses and patient positions, avoiding the need for power and signal cables.

The ZigBee network is introduced in the proposed platform to increase the reception coverage area, to provide sufficiently high transmission rates for high-resolution ECG signals and for node management (until 65k nodes can be used with low-power features). Furthermore, the ZigBee network can use router nodes to expand the coverage area or introduce several topologies, depending on application needs. The proposed solution provides targeted emphasis to the HC enclosure to ensure proper conditions inside the HC where there is a high concentration of $HBO_2$.

Table 1 summarizes a comparison of the main features of the existing wireless platforms. The numbers represent

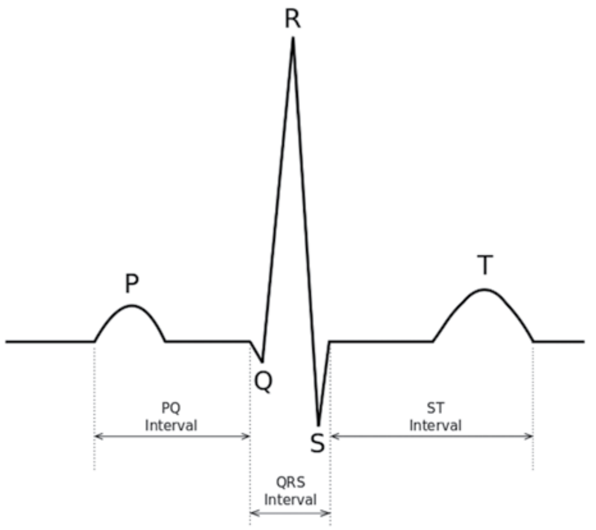

**FIGURE 2.** ECG signal model with the five waveform sections

the order of solutions considering the different features and constraints in hyperbaric chamber applications.

The next section analyzes the system design and gives an overview of the HC features and a description of the ECG signal. Section 3 discusses the main benefits of indoor wireless nodes and reports the battery consumption experimentally obtained for the proposed approach. Indoor node firmware issues are analyzed in Section 4, while Section 5 presents the implementation details and the experimental results obtained for the proposed approach. Finally, some conclusions are given.

## 2 HYPERBARIC CHAMBER APPLICATION ISSUES

### 2.1 Hyperbaric chamber overview

A hyperbaric chamber is basically a metallic-walled room with very small windows where the patient is exposed to a higher-than-atmospheric pressure. Figure 1 shows two views of the HC used at Perpetuo Socorro Hospital (Alicante, Spain) to apply $HBO_2$ treatment. The main HC feature is metal the walls (e.g., the thickness of the HC metal walls in Figure 1 is 12 mm) and creates a "Faraday cage" effect, which causes coverage reduction and low-quality signal at the receiver antenna.

The wireless communication is not fully affected by this Faraday cage effect because the HC has methacrylate windows (with a thickness of about 40 mm) used to observe the patients from outside. Those small methacrylate windows essentially "break" the Faraday cage formed by the HC walls, and although producing a significant coverage area reduction, the communication link between internal devices and the external receiver can be maintained with sufficient signal quality while adjusting power consumption levels.

Another important issue to take into account when designing electronic devices for HC applications are the inside conditions. During the application of hyperbaric treatment, the interior of the HC is typically pressurized from 1.7 to 6 atmospheres, depending on the specific treatment, although the most common pressure is 2.5 atmospheres. Electronic devices working inside the HC have to fulfill specific regulations (Directives 2006/95/EC [12], 93/42/EEC [13] and 97/23/EC [14] of the European Parliament and of the Council) that mandate proper enclosures and components for the electronic devices.

The main challenge faced in hyperbaric monitoring is to maintain a sufficiently high resolution signal at the external receiver for obtaining medical diagnostics. The selected communication protocol is based on the ZigBee Stack because of its maximum transmission velocity (higher than Bluetooth but lower than WiFi) and the low-power transmitter, enabling the use of in-chamber devices with battery power supply.

### 2.2 Biological parameters

The designed platform communicates the following vital signs: ECG, body temperature ($bT^a$) and $TcPO_2$ (transcutaneous oxygen pressure) signal.

ECG is the most complex signal due to the number of wave sections and the signal frequency components. Typically, five parts describe the ECG waveform: P, Q, R, S and T. Figure 2 identifies each waveform section corresponding to different electrical potentials related to cardiobehavior. The five ECG waveforms are reproduced periodically at cardio-frequency and have different time duration and frequency components depending on the patient. In terms of high-frequency components, the most complex section is the QRS interval [15].

Compared to ECG, the variations of others biosignals are slower. Therefore the A/D (analog-to-digital) conversion period (T = 1/2 Khz = 0.5 ms) is more than enough to sample the ECG signal (T < 1/250 Hz = 4ms). The body temperature, $TcPO_2$ or other signals (up to three) are digitalized in parallel with the ECG signal, maintaining the same conversion time period. Any kind

| signal | definition | voltage | frequency |
|---|---|---|---|
| ECG | electrocardiography | 0.5-4mV | 0.01-250Hz |
| EEG | electroencephalography | 5-300µV | DC-150Hz |
| EMG | electromyography | 0.1-5mV | DC-10KHz |
| EOG | electrooculography | 50-3500µV | DC-50Hz |
| bT$^{a}$ | body temperature | 0-5mV | DC-0.1Hz |
| PCG | phonocardiography | 0.5-4mV | 5-2000Hz |
| ENG | electroneuronography | 0.01-3mV | DC-1KHz |
| TcPO$_2$ | transcutaneous oxygen pressure | 0-10mV | DC-0.1Hz |

**TABLE 2.** Features of biosignals

of biological signal could be transmitted if the bandwidth constraints and voltage constraints are accomplished. Table 2 shows the features of some biosignals. The system designed and implemented in this project can transmit up to 2 kHz and a maximum of four devices, i.e., biosignals. Therefore a feasible set of configurations could be: {ECG, EEG, EOG, bT$^{a}$}, {ENG, bT$^{a}$, EOG, EMG}, {PCG, -, -, -}. Moreover, the system is able to connect a few tens of patients with the central collector or gateway device. However, if the ZigBee Pro is considered, its ad hoc on-demand distance vector (AODV) [16] for routing across a mesh network would allow to connect more than 40 patients at the same time.

To optimize the resolution of the A/D converter, the value of the voltage reference ($V_{REF}$) (shown in Figure 3) should be slightly higher than the maximum value of the voltage converted by the PIC. Attending to Table 1, it would be 5mV if EMG or bT$^{a}$ are transmitted. The resolution of the system will be res = $V_{REF}$/ 210, e.g., res = 5mV/210=4.9µV (Note that, in general, $V_{REF}$ may be larger that the maximum voltage of the biosignal, but in that case resolution gets worse).

The ECG signal is obtained from the voltage difference between the contraction and relaxed states of the heart muscle, which is around 90mV (≈-70mV in a relaxed state and ≈20mV in a contraction [17]). This voltage difference is theoretically obtained from the measurement at the myocardium. However, the ECG system uses electrodes located on the skin surface with several fat and skin layers between myocardium and electrodes, so the initial values are attenuated until to a range of 5mV/-5mV [18]. An analog front-end circuit adapts the ECG differential signal to the A/D converter input. The front-end circuit consists on three stages (see the wiring diagram in Figure 3 and the actual implementation in Figure 4). A pre-amplifier stage is the first step to obtain a voltage gain of 10 with high CMRR and low noise input. The second state is a low-pass Sallen-Key filter with a cutoff frequency of 100Hz and damping ratio of 0.2 dB. The final stage is a post-amplification using an inverter amplifier with voltage gain of 30.

Each stage is responsible of different functions:

- The pre-amplification stage eliminates the influence of other physiological signals on the ECG sensor like the voltage induced by muscle movements or the patient skin surface tension. This is achieved using a differential measurement at three points: two of them connected to the differential inputs of the amplifier and the last one used as stage reference node.
- The low-pass filter stage is able to remove the high-frequency noise components of the signal with no significant attenuation of the signal.
- The post-amplification stage removes the negative voltage values of the input signal, adding a positive offset voltage (1.5V) and causing the output range to move from [-1.5...1.5 V] to the range [0...3 V].

Thus, the analog front-end stages amplify the ECG input signal by a total voltage gain of 300: The initial voltage range of 10mV (+ 5mV) is converted to the voltage range [0...3 V], which is the input to the A/D converter.

Similarly, the capnometry device, the body temperature sensor and the TcPO$_2$ signals are adapted to the A/D converter input range to obtain adequate resolution. In these cases the analog front end consists of an amplifier stage with unit voltage gain and a similar low-pass Sallen-Key filter. These signals do not require amplification because the sensor outputs are in the voltage range of the A/D converter that is used.

## 3. THE PROPOSED PLATFORM

The proposed system is based on a wireless sensor network using the ZigBee protocol to perform the network management between the nodes inside the HC and a receiver module outside the HC (see Figure 5). The nodes inside chamber (NICs) elements are battery-powered and perform signal conditioning. They are connected to patients through individual body sensors. The external device acts as a coordinator node in the ZigBee network

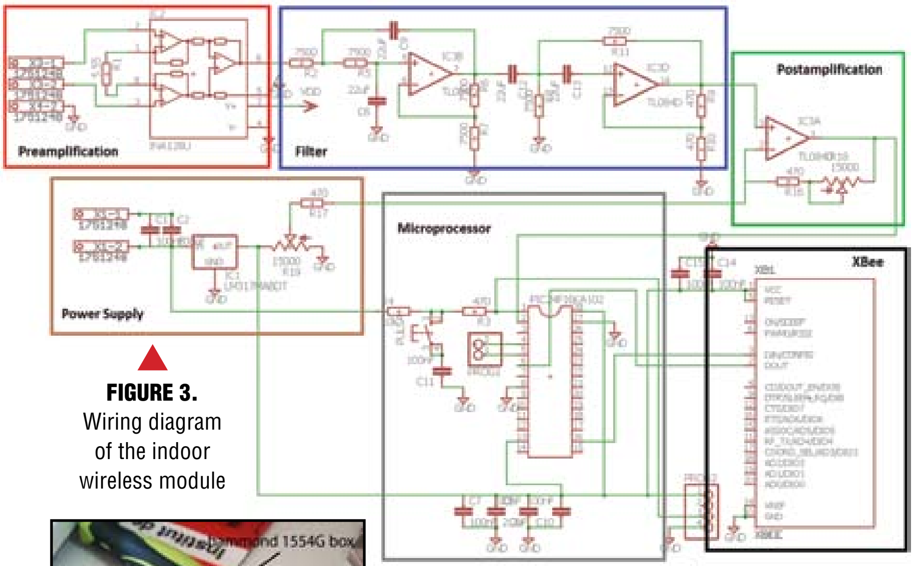

**FIGURE 3.** Wiring diagram of the indoor wireless module

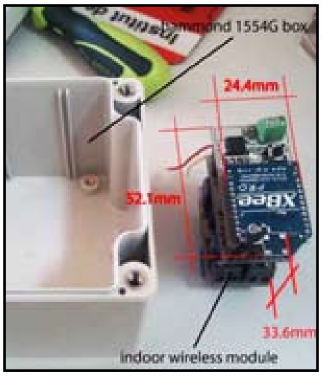

**FIGURE 4.** Actual implementation of the indoor wireless module

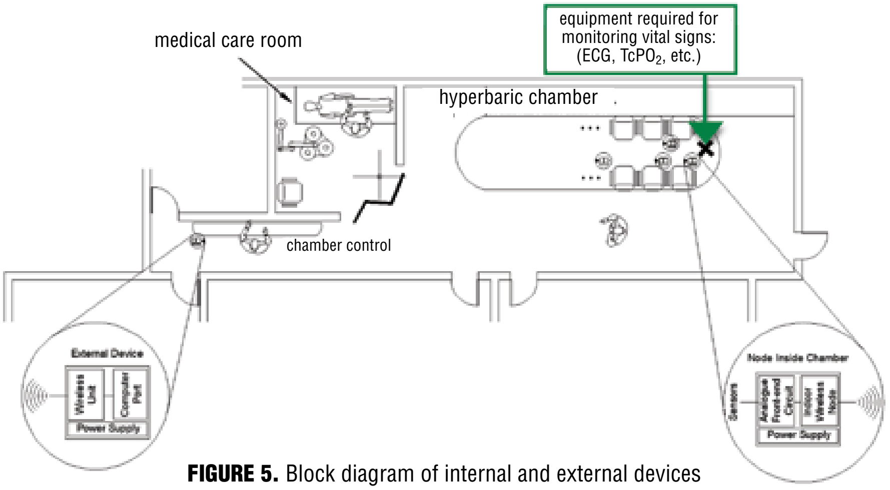

**FIGURE 5.** Block diagram of internal and external devices

and is a real-time receiver module. This device is plugged to a computer representing the HC Control System. The ZigBee protocol allows several useful features:

- The NICs are instantaneously incorporated into the network and data are sent immediately because the network allows broadcasting mode. This minimizes the data frame overhead and uses a transmission channel shared between all nodes with no priority definition.
- The wireless network has a maximum transmission rate of 250 Kbps, which allows monitoring of several patients at the same time. Although the number of NICs per network is limited by the transmission rate, several networks can be considered using different identifiers and frequency channels (ZigBee protocol allows up to 16 frequency channels) in order to increase the number of patients being monitored, if needed.
- The ZigBee protocol allows the inclusion of router nodes to change network topology and to expand the initial coverage area without reducing the transmission capabilities of the network.

In addition, the ZigBee protocol was selected due to its easy integration with commercial devices or such applications as home health monitoring.

### 3.1 The node inside the chamber

Two main parts form each NIC: the analog front-end circuit for sensor outputs adaptation and the indoor wireless module (see Figure 3). The indoor wireless module is a microcontroller-based circuit, which performs three functions: the A/D conversion, the implementation of the defined communication frame and the transmission process using the ZigBee protocol.

The enclosure adopted in this proposal is the Hammond 1554 G box, which complies with the hermetic protection requirements of HC regulations [12-14]. The added connectors maintain the hermetic protection using internal plastic barriers. The power supply is based on AA batteries, allowing easy substitution and the use of rechargeable units.

The indoor wireless module is designed to use an XBee transmitter (XBee is a specific implementation of the ZigBee standard protocol) because it offers power consumption control and has sufficient transmission rate (250 Lbps) to support several patients in the same network. The battery performance is important to determine if the proposed system is useful to monitor a complete $HBO_2$ treatment, which lasts around two or three hours. The other important subsystem present in the indoor wireless module is the microcontroller (from Microchip), which performs the A/D conversion of four analog inputs (one for each monitored vital sign): ECG, capnometry sensor (if needed), body temperature ($bT^a$) and $TcPO_2$. The general-purpose Microchip microprocessor chosen was PIC24F16KA102, which is a 16-bit microcontroller that has an internal 10-bit high-speed A/D converter with a maximum conversion speed of 500 Ksps.

To minimize the power consumption, a specific test has been performed to measure the current waveform during transmission/reception of data. To get information about consumption and timing, a 4.9-Ω shunt resistor is connected between the voltage supply and the input of the module. States of the device can be seen in Figure 6. In RX mode, the device is listening via the communication channel; its consumption is minimum with the device in enable mode. The TX mode requires activation of the transmitter; consumption is maximum. Changes between RX and TX modes require turning off the radio circuit. The XBee module has the lowest consumption current value of them all.

## 4. FIRMWARE

The NIC firmware not only performs communication tasks but also performs the conversion of analog signals to digital and creates the data frame to be transmitted to the external device. All of these functions have an impact on system performance because they are time-conditioned. Therefore, a precise time schedule must be defined to reduce unnecessary delays. Figure 7 shows the time diagram defined using an oversampling strategy [19] where *input* (N) denotes each analog input and *sample* (N) the sample number (with N = 1, 2, 3 or 4).

The proposed methodology establishes two different independent processes with different time configurations:

- the A/D conversion process, which defines the sampling frequency of each analog input signal;
- the communication process according to the maximum transmission rate.

The timing pattern of A/D conversion process is established considering that each analog input signal is sampled four consecutive times at the minimum sampling period of 2μs (i.e., 500 K samples per second). Therefore, considering four different analog inputs, the same input signal is sampled using a conversion period,

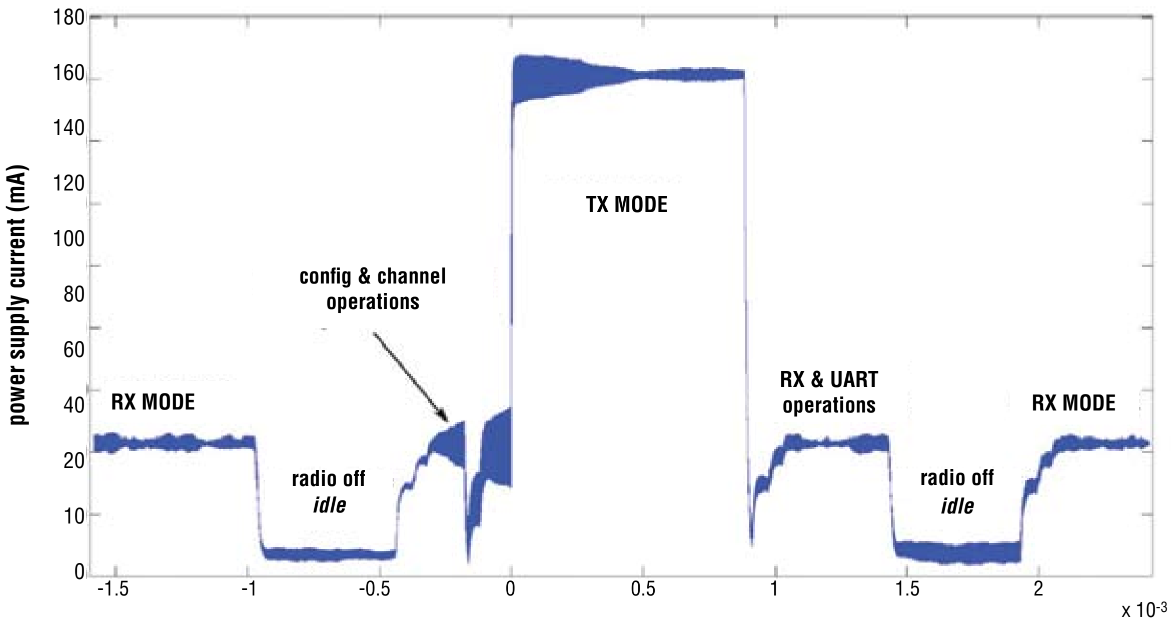

**FIGURE 6.** Measured supply current of XBee module during the transmission and reception of data

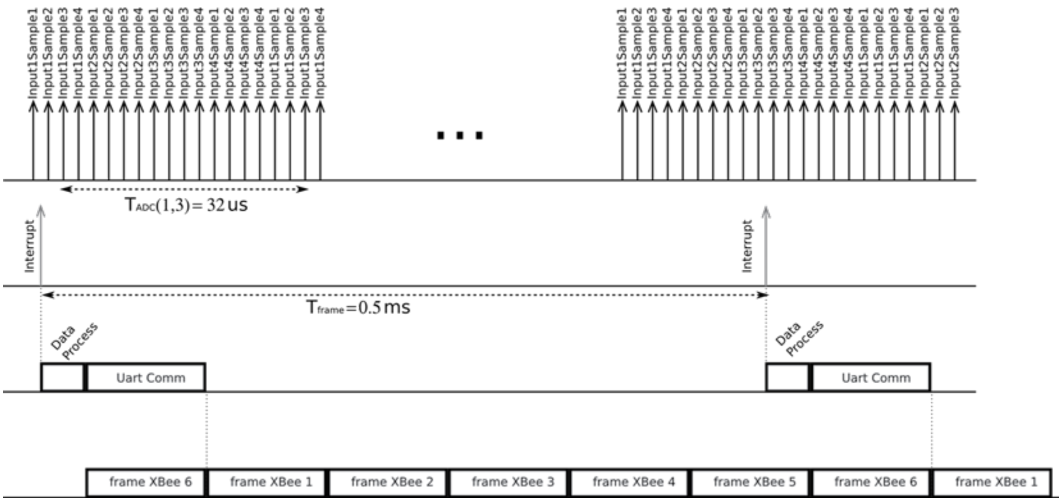

**FIGURE 7.** Transmission timing diagram

namely $T_{ADC}$, of 32µs (see Figure 7). As a result, a total of 16 samples from four analog signals are stored in the ADC buffer waiting to be transmitted. The continuous conversion strategy uses a rotation scheme that, after the sixteenth sample is stored (input4sample4 in Figure 7), a new rotation updates the A/D converter buffer with a new value (input1sample1 in Figure 7), then the second sample (input1sample2) and so forth. The samples stored in the A/D converter buffer are used to calculate the average value of the last four sampled values for the same signal and, hence, smooth sample variability is achieved.

Independently of the previous rotation conversion time, the main program is working on communication

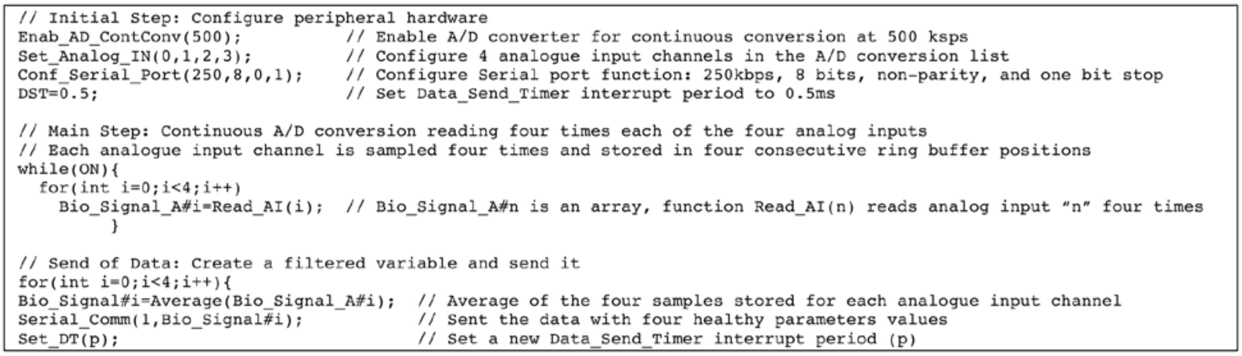

```
// Initial Step: Configure peripheral hardware
Enab_AD_ContConv(500);          // Enable A/D converter for continuous conversion at 500 ksps
Set_Analog_IN(0,1,2,3);         // Configure 4 analogue input channels in the A/D conversion list
Conf_Serial_Port(250,8,0,1);    // Configure Serial port function: 250kbps, 8 bits, non-parity, and one bit stop
DST=0.5;                        // Set Data_Send_Timer interrupt period to 0.5ms

// Main Step: Continuous A/D conversion reading four times each of the four analog inputs
// Each analogue input channel is sampled four times and stored in four consecutive ring buffer positions
while(ON){
  for(int i=0;i<4;i++)
    Bio_Signal_A#i=Read_AI(i);  // Bio_Signal_A#n is an array, function Read_AI(n) reads analog input "n" four times
         }

// Send of Data: Create a filtered variable and send it
for(int i=0;i<4;i++){
Bio_Signal#i=Average(Bio_Signal_A#i);  // Average of the four samples stored for each analogue input channel
Serial_Comm(1,Bio_Signal#i);           // Sent the data with four healthy parameters values
Set_DT(p);                             // Set a new Data_Send_Timer interrupt period (p)
```

**FIGURE 8.** Extract of pseudocode incorporated into the indoor wireless module

tasks, i.e., defining the data frame and sending it to the wireless transmitter. The data frame is transmitted with a frequency rate of 2kHz. Each frame contains the average values of four vital signals. Figure 7 represents how the data frame is defined at each T-frame using an internal interrupt generated at a fixed period, which acts as effective sampling frequency of four analog signals. As a consequence, the transmission channel is divided on T-frame time windows where each NIC node can send its data frame with no conflict with the other NICs sharing the same SSID network. The horizontal axis at the bottom of Figure 7 represents the time division of the transmission channel given by T-frame.

There are two relevant issues to understand the continuous rotation sampling strategy:

- The sampling period $T_{ADC}$ (see Figure 7) is shorter than the transmission period T-frame. This sampling period minimizes the voltage differences between the four sample values of each analog signal and can be considered sampled at the same instant of transmission.
- The sampling process and the transmission process work independently and in a continuous cycle. Due to this independency, the time delay between the four samples of each signal could not be equal. Therefore, some samples could be converted at the present cycle and the rest at a previous cycle. This introduces an extra sampling delay between samples of 32μs (16 samples /500 Ksps). The averaging function reduces the impact of this extra sampling delay on signal reconstruction and smooths out the presence of conversion noise.

The time scheme shown in Figure 7 has been implemented at the firmware of each NIC microcontroller. To perform the described time strategy, two different tasks (transmission and conversion) run in parallel. In this sense, the NIC firmware has been designed using an interrupt-based programming strategy developing an event-based programming code. The main steps implemented by NIC firmware are shown in Figure 8.

This code runs inside the microcontroller depicted in Figure 3, while the final device implementation is shown in Figure 4. Note that all electronics are around 52.1mm x 24.4mm x 33.6mm in size and are introduced inside a special box (Hammond 1554G) with the battery pack.

The number of patients with NIC devices is an important feature of the proposed platform. The estimated number of NICs that will be able to communicate with the receiver module must take into account the NIC broadband transmission mode and the time division of the transmission channel discussed above. With this consideration, the wireless transmitter is configured to use the maximum transmission rate allowed by the ZigBee network – i.e., 250 Kbps. In this context, the maximum number of NICs will be limited by the frame overhead and the frequency delay between each frame. Therefore, considering that the broadcast mode reduces the frame overhead extension to minimum and has a frequency delay between frames of 2kHz, the maximum number of patients with NIC is established as six patients per network. Thus, using all frequency channels, the maximum number of patient with continuous monitoring results in 96 patients (16 channels x 6 patients). This number is large enough since the number of available seats is the HC is below that number.

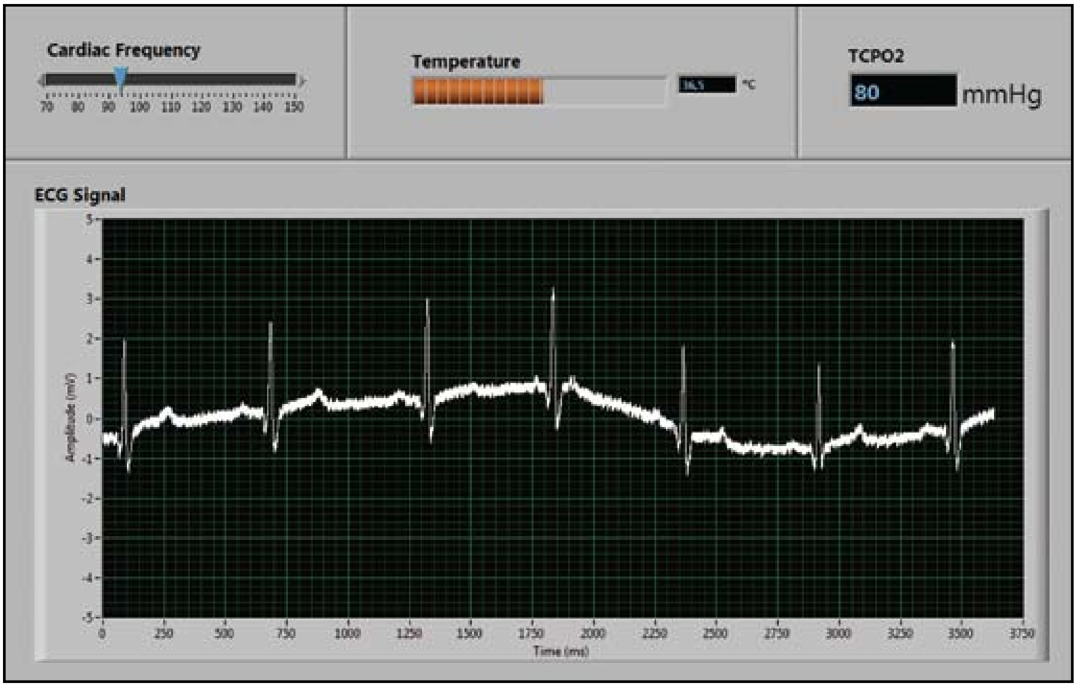

**FIGURE 9.** LabView-based user interface

## 5. IMPLEMENTATION AND PERFORMANCE RESULTS

### 5.1 User interface

The device located outside the HC acts as the network root and receives information from the NICs. The data received are shown on a computer-based user interface (UI) with a large number of processing and representation options, which allows a detailed analysis of the data collected during the sessions. In particular, a chamber control UI has been developed using a LabView application, which captures and processes the signal data from all NICs. The UI configures the reception port, shows both the raw data and the graphic representation and stores the received data in a plain text file for post-analysis purposes.

The information from each NIC sensor is extracted from the received raw data frame. This information is processed to determine the sensor values; those values are displayed on screen in real-time. Figure 9 shows the UI designed with Labview. Each sensor data are displayed with different graphical objects. For instance, the graphical representation of the ECG signal shows the waveform information with no processing. The horizontal axis represents time, while the vertical axis represents the differential voltage value measured by the instrumentation amplifier over the patient's skin. The waveform interface allows zoom-in and zoom-out operations to observe in detail any part of the ECG waveform, if needed. The cardiac frequency is obtained from the ECG signal evaluating the delay between peaks, while the body temperature and the $TcPO_2$ value are obtained directly from received data.

The system noise response is analyzed via testing for different work environments and quantifying the influence of external noise on the obtained data. The quality of the signal is accurate enough to determine heart anomalies. To preserve the ECG signal from noise there are two important factors to take into account: the sensor placement and the sensor contact surface – e.g., there is a drift in the middle voltage for surfaces with poor contact.

### 5.2 Platform coverage

The coverage of the proposed system has been evaluated in the HC environment of the Perpetuo Socorro Hospital in Alicante (Spain). Figure 10 shows coverage results estimation with the NIC prototype located in the HC and the external device used to define the quality reception signal map. The coverage area allows reception of the information in multiple places (shaded

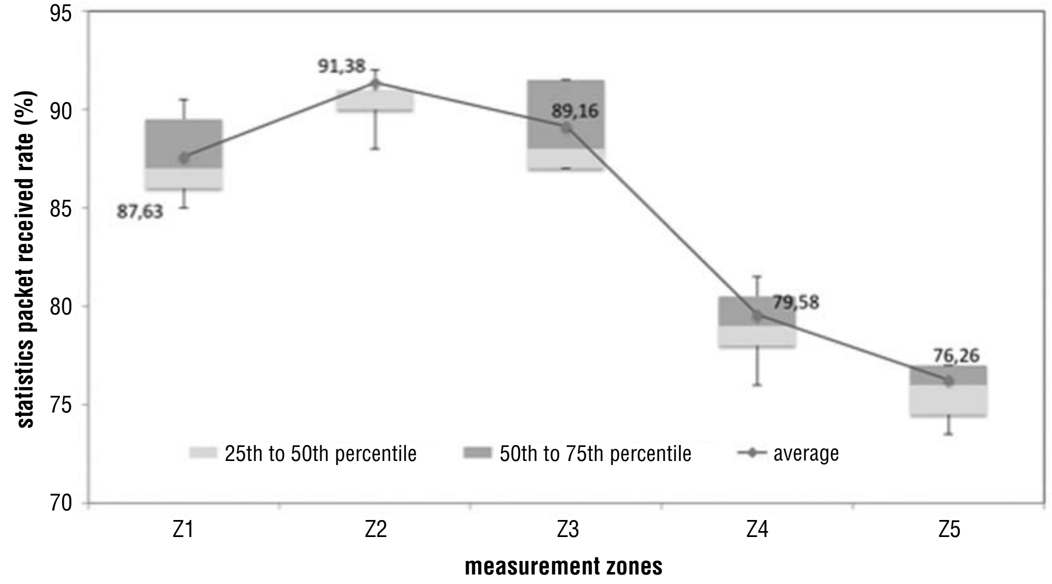

**FIGURE 10.** Statistics of packed received rate at different locations in the hospital facilities

area of Figure 11): from the HC control office to the observation cabin. To overcome the thickness of the constituent material of the windows, the lowest power transmission is estimated to 2mW.

The distribution example shown in Figure 11 is a worst-case scenario: in this case, the NIC location was in the farthest corner of the HC, while the receiver was located in the opposite corner of the room. In fact, coverage is better near the NIC and in the direct line of vision through the windows, while it decreases rapidly when the receiver is moved diagonally and direct sighting through the windows is lost.

Several locations shown in Figure 11 have been evaluated – namely Z1-Z5. Packed received rate (PRR) statistics have been measured for each Zn point maintaining the NIC device at the same position. The NIC position is indicated in Figure 11 as "ECG device to test." Figure 10 shows that the maximum PRR is obtained near the hyperbaric chamber control zone (Z2) due to the position of the methacrylate windows. Note also that the link signal quality plummets when the receiver is located in a direction diagonal to direct sight through the hyperbaric chamber windows (positions Z4 and Z5).

### 5.3 NIC power autonomy

The power supply for each NIC consists of batteries that must meet the system power requirements and autonomy for the application. To fulfill these requirements, the voltage levels and the maximum currents must be specified. The system requires three different voltage values. The maximum positive voltage value (+6V) powers the analog front-end circuit. The minimum positive voltage value (3.3V) powers the microcontroller and transmitter circuits. Negative voltage (-6V) is required for the inverter amplifier, to provide a negative output by means of a positive input.

Regarding the power supply requirements, the maximum consumption measured on each NIC is 125mA. The typical $HBO_2$ treatment lasts between 60 and 120 minutes. Therefore, the power supply source for each NIC consists of four AA batteries with 1.5V of nominal voltage and a minimum capacity of 700mAh. This pack of batteries is 63mm x 58mm x 17mm in size (cells have a weight of roughly 92g), a reduced size that can be carried easily by the patient. The capacity of the batteries was tested connecting a regulated load, recording the time until the output voltage falls

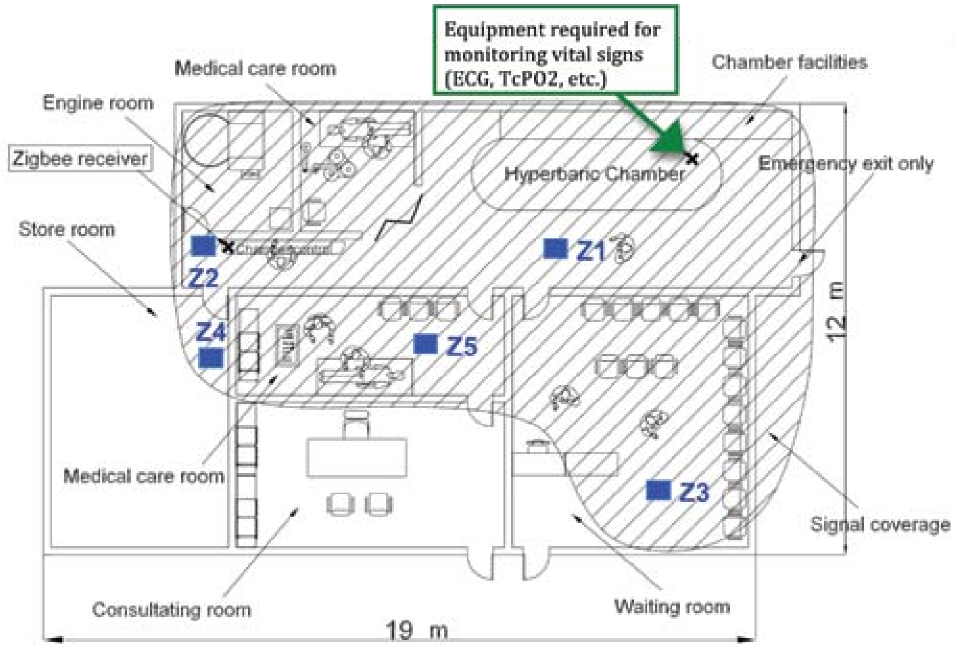

**FIGURE 11.** Schematic representation of the hospital facilities showing the signal coverage for the NICs

below the cutoff voltage of the system, estimated as 3.8V. Figure 12 shows the batteries' voltage response with respect to time. The measurements indicate that the capacity of the battery produces an average autonomy of about six hours beyond the initial requirements.

### 5.4. Equipment

The components from manufacturers used in this work are detailed below:

- controller: Microchip PIC24F16KA102.
- ECG electrodes: VERMED A10005 Wet Gel. The electrodes are directly connected to the homemade signal conditioning system and, hence, no electrocardiograph is required in this case.
- bT$^a$ sensor: an original equipment manufacturer (OEM) version of the PCE-FIT 10 forehead thermometer has been used. The electronics are placed inside the NIC box while the temperature electrode is attached to the patient's body.
- TcPO$_2$ sensor: Periflux 6000. In this case, Perimed supplied the machine and electrodes.
- wireless communication hardware: XBee Pro 2 supplied by Digi International (www.digi.com); it is equipped with its own antenna and is ready to use.
- The wiring schemes for the homemade signal conditioning are shown in Figure 3.

It is important to remark that the ZigBee network represents a general-purpose wireless transmission system to be used inside the HC. In some cases (e.g., bT$^a$ or TcPO$_2$), the equipment required for monitoring the patient vital signs will need to be in the HC with the ZigBee node (see Figures 5 and 11). In other cases (e.g., ECG or EMG), the node is completely autonomous – i.e., electrodes are connected directly to preamplification inputs, as shown in Figure 3. Therefore, such equipment (commercial and implemented in this project) would need to be tested and approved for use inside the HC since we are adding equipment inside that is usually outside.

### 5.5. Chamber pressure

Figure 13 shows the HC pressure profile considered for the tests. Note that the most common pressure of 2.5 atmospheres for HBO$_2$ treatments has been considered.

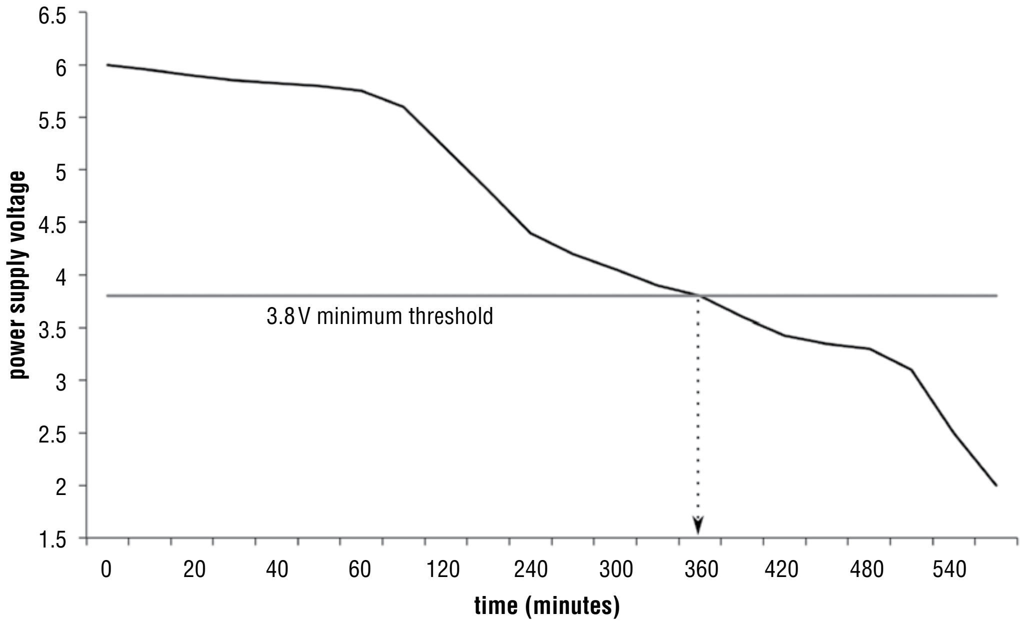

**FIGURE 12.** Battery voltage level vs. time
The minimum value allowed by the system gives an autonomy of around six hours

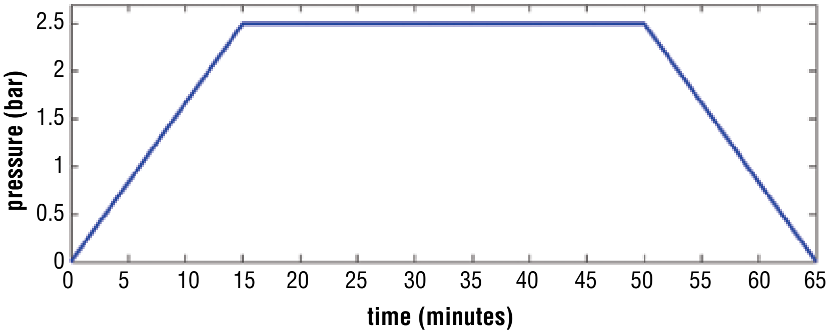

**FIGURE 13.** Chamber pressure profile used for the tests

However, the enclosure used for the NICs (Hammond 1554 G box) complies with the protection requirements of HC regulations [12-14] and could be used with a pressure of up to 6 atmospheres. The profile in Figure 13 has been used with the developed NICs together with the ECG electrodes and bTª sensor inside the chamber. For the case of the TcPO2, the tests were conducted with the chamber not pressurized since this equipment is not specially designed for hyperbaric environments (see Section 5.4). Note that this work is focused on the wireless transmission system and, hence, this is the main device to be analyzed. Anyway, as indicated above, all the equipment (commercial or self-developed) to be used inside the HC has to fulfill the corresponding regulations to work in hyperbaric conditions.

### 5.6. Patient privacy

First of all, note that the coverage area of the ZigBee system is around few meters and hence, the signal can be received only near the HC (see Figure 11). Furthermore, no personal information is transmitted using the proposed system – i.e., only the sensor data are sent through the network. Hence all data remain anonymous. In order to improve the transmission speed, no kind of encryption can be used in this work for transmitting data. However, to help improve privacy data encryption could be used. For instance, this should be considered before commercializing the proposed system. This is out of the scope of this paper, however, and remains as further work.

## 6. CONCLUSION

This work has developed a platform based on the ZigBee network to use wireless technology for monitoring vital signs in HC applications. The system has been designed taking into account the conditions of the HC environment and with the following main objectives:

- Low power consumption, in order to reduce battery size and to obtain a wearable device.
- Low cost, since the hospital expects to use this device heavily, and the average life of each one will likely be limited.
- Real-time monitoring, in order to allow the medical staff to see the complete ECG signal in real time via their tablets or smartphones.
- Pressure resistance, in order for the devices to support up to 6 atmospheres, which is the typical maximum pressure in $HBO_2$ treatments.

The main advantages of the wireless transmission system designed and implemented in this work are:

- Its size is small (see Figure 4), improving the patient's mobility. Note that the system can be considered wearable if only the ECG is transmitted.
- Its price is significantly lower than the traditional option, e.g., a commercial hyperbaric ECG with telemetry capabilities.
- It allows simultaneously transmission of the signals from several different sensors: e.g., ECG, bTª, $TcPO_2$.

Finally, to illustrate the applicability of the proposed approach, the platform developed has been tested experimentally and analyzed in the Perpetuo Socorro Hospital, located in Alicante, Spain.

■

**Acknowledgment**

The authors would like to thanks the University of Balearic Islands (UIB), the Miguel Hernandez University (UMH), MEDIBAROX unit of the Perpetuo Socorro Hospital (Alicante, Spain) and the "Catedra de Medicina Hiperbarica" for its support and allowing the use of its facilities for this work. We would also like to thank Borja Mas Boned for his help designing the capture application.

**Conflict of interest statement**

Authors declare no conflicts of interest exist with this submission.

## REFERENCES

1. Brubakk AO. Hyperbaric oxygen therapy: oxygen and bubbles. Undersea Hyperb Med. 1995; 31: 73-79.
2. Mutluoglu M, Metin S, Arziman I, Uzun G, Yildiz S. The use of hyperbaric oxygen therapy for carbon monoxide poisoning in Europe. Undersea Hyperb Med. 2016; 43: 49-56.
3. Memarpour R, Tashtoush B, Nasim F, Grobman D, Upadhyay BK, Rahaghi F. A deep-sea diver with cement pulmonary embolism. Undersea Hyperb Med. 2016; 43: 249-255.
4. Gesell LB. Hyperbaric oxygen therapy indications: the hyperbaric oxygen therapy committee report. Undersea and Hyperbaric Medical Society. 2008.
5. Lin BS, Chou NK, Chong FC, Chen SJ. RTWPMS: A real-time wireless physiological monitoring system. IEEE Trans Inf Technol Biomed. 2006; Oct; 10(4):647-656.
6. Hu S, Wei H, Chen Y, Tan J. A real-time cardiac arrhythmia classification system with wearable sensor networks. Sensors 2012; 12: 12844-12869.
7. Burns A, Greene BR, McGrath MJ, O'Shea TJ, Kuris B, Aye SM, Stroiescu F, Cionca V. SHIMMER™ – A wireless sensor platform for non invasive biomedical research. IEEE Sensors Journal 2010; 10: 1527-1534.
8. Gil Y, Wu W, Lee JA. Synchronous multi-body sensor platform in a wireless body sensor network: design and implementation. Sensors 2012; 12: 10381-10394.
9. Lin CT, Chang KC, Lin CL, Chiang CC, Lu SW, Chang SS, Lin B, Liang HY, Chen RJ, Lee YT, Ko LW. An intelligent telecardiology system using a wearable and wireless ECG to detect atrial fibrillation. IEEE Transactions on Information Technology in Biomedicine 2010; 14: 726-733.

10. Chung WY, Lee YD, Jung SJ. A wireless sensor network compatible wearable U-healthcare monitoring system using integrated ECG, accelerometer and Spo2. Conf Proc IEEE Eng Med Biol Soc. 2008: 1529-1532.

11. ZigBee Alliance. http://www.zigbee.org/ (accessed January 2017).

12. Directive 2006/95/EC of the European parliament and of the Council. (12 December 2006).

13 Directive 93/42/EEC of the European parliament and of the Council. (14 June 1993).

14. Directive 97/23/EC of the European parliament and of the Council. (29 May 1997).

15. Akay M. Time frequency and wavelets in biomedical signal processing. IEEE Press Series in biomedical Engineering 1998; 28:739.

16. Large ZigBee Networks and Source Routing. http://www.digi.com/wiki/developer/index.php?title=Large_ZigBee_Networks_and_Source_Routing&amp;redirect=no (accessed January 2017).

17. Tortora GJ, Derrickson B. Principles of anatomy and physiology. 12th ed. John Wiley & Sons, NJ, 2009:729.

18. Fauci AS, Wiener C, Bloomfield G, Harrison TR. Harrison's principles of internal medicine: self-assessment and board review. 17th ed. McGraw-Hill, New York, 2008.

19. Marks RJ. Introduction to Shannon sampling and interpolation theory. Springer-Verlag, New York, 1991; xiii:324.

✦